

Fire Plume Rise Model Introduction

Jianfeng Li, Ziming Ke

Background

- Fire smoke: human health, visibility, air quality, regional climate change.

Predicting the smoke effects of wild-land fires

1. Description of the emissions source, include both pollutants and heat release.
2. Determination of plume rise through atmosphere's stability and wind profiles
3. Movement of the smoke by the ambient wind
4. Chemical transformations with ambient atmosphere

Plume rise and air quality models & schemes

- Box model: Ventilated Valley Box Model (VALBOX)
- Gaussian plume model: VSMOKE, SASEM
- Puff model: CALPUFF, HYSPLIT
- Particle model: FLEXPART, DaySmoke, PB-Piedmont
- Eulerian grid model: CMAQ, WRF-Chem
- Full physics model: Active Tracer High-resolution atmospheric model (ATHAM), ALOFT

Wild-land fire plume rise scheme
developed by M. Sofiev, T.
Ermarkova and R. Vankevich (MER)

Briggs stack plume rise scheme (1)

- Start from buoyancy flux and momentum flux, combined with dimensional analysis, fitting empirical formulas for stack plume rises under different conditions.

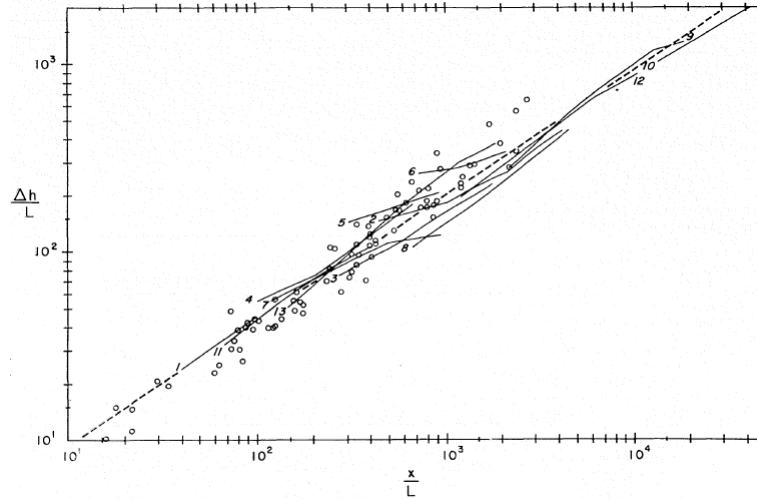


Fig. 1. Observed plume rises vs $\Delta h = 2.0F^{1/3}U^{-1}x^{2/3}$ (dashed line).

$$H_c = \begin{cases} 1.6F^{1/3} (3.5x^*)^{2/3} U^{-1} \\ 2.4(F/Us)^{1/3} \\ 5F^{1/4} s^{-3/8} \end{cases} = \begin{cases} \begin{cases} 21.4F^{3/4}U^{-1}, & F < 55m^4s^{-3} \\ 38.7F^{3/5}U^{-1}, & F \geq 55m^4s^{-3} \end{cases} & \text{Neutral, unstable} \\ 2.4(F/Us)^{1/3} & \text{stable, } U > 0.5m s^{-1} \\ 5F^{1/4} s^{-3/8} & \text{stable, } U \leq 0.5m s^{-1} \end{cases}$$

$F = gv_s r^2 (1 - \rho_p / \rho_a)$ is buoyancy flux parameter

$s = \frac{g}{T_a} \frac{\partial \theta}{\partial z}$ is buoyancy parameter

Where H_c is final rise of the plume centerline from the stack top, g is acceleration due to gravity, v_s is stack gas exit velocity, r is stack exit radius, ρ_a is ambient air density, ρ_p is plume density, x^* is distance at which the atmospheric turbulence begins to dominate over the entrainment, U is mean horizontal wind speed averaged from the top of the stack to the top of the plume.

Briggs stack plume rise scheme (2)

$$H_c = \begin{cases} 2.1 \left(\frac{rv_s^3}{N^2 \Phi^2 U} \right)^{1/3} \\ 0.76 \left(\frac{rv_s^3}{u_*^2 \Phi^2 U} \right) \\ 4.5 \left(\frac{rv_s^3 z_i^{2/3}}{4w_*^2 \Phi^2 U} \right)^{3/5} \end{cases}$$

$\Phi = v_s / \sqrt{gr(1 - \rho_p / \rho_a)}$ is the Froude number

N is the Brunt-Väisälä frequency, u^* is the friction velocity, w^* is the convection scale velocity, z_i is the height of the nearest inversion layer above the stack stop

$$N \equiv \sqrt{\frac{g}{\theta} \frac{d\theta}{dz}}$$

Brunt-Väisälä frequency, or buoyancy frequency, is the angular frequency at which a vertically displaced parcel will oscillate within a statically stable environment.
 (http://en.wikipedia.org/wiki/Brunt%E2%80%93V%C3%A4is%C3%A4l%C3%A4_frequency)

Weak point: assume a vertically-homogeneous atmosphere, which can be described via some parameters at the top of the stack; require diameter of the buoyant plume at the stack top, temperature and velocity of the outgoing gas, gas density, etc.

MER wild-land fire plume rise scheme

Assumption: The heat energy of the fire is spent only against buoyancy forces.

Change the criterion for the end of the rise: the plume comes to equilibrium with the surrounding air when the energy excess pumped into it by the fire is fully spent in the uplift.

Available data: {

- MODIS (Fire Radiative Power) FRP
- Operational archives of the European Centre for Medium-Range Weather Forecast (ECMWF)

MER scheme derivation (1)

** Consider only two processes: the uplift against the atmospheric stratification and the plume widening due to entrainment of the surrounding air.

Let the fire energy E_0 be pumped into an air volume V while it is in contact with the flames. Then the density of the energy excess e_0 in comparison with the undisturbed surrounding air will be:

$$e_0 = \frac{E_0}{V} = \frac{E_0}{S_f w \tau} = \frac{P_f}{S_f w}$$

w is the initial mean vertical velocity of the plume, τ is the time period during which the volume is in contact with flames, S_f is the fire area (of any shape), P_f is the fire power released into the air.

MER scheme derivation (2)

The initial energy excess can be expressed in terms of difference of initial temperatures of the plume T_p^0 and ambient air T_a^0

$$e_0 = c_p \rho_a (T_p^0 - T_a^0)$$

Where c_p is specific heat capacity at constant pressure of air, ρ_a is air density.

If the plume rises adiabatically

$$\frac{d(T_p - T_a)}{dz} = - \frac{d\theta}{dz}$$

The change of the energy excess $e(z)$ during the uplift can be written as:

$$\frac{de}{dz} = -c_p \rho_a \frac{d\theta}{dz} - \frac{E_0}{V^2} \frac{dV}{dz}$$

The first term characterizes the change of the temperature difference between the plume and ambient air, whereas the second term reflects plume widening.

MER scheme derivation (3)

$$\frac{d\sigma^2}{dz} = \frac{2K_{hor}}{w}, \quad \Rightarrow \quad S = \pi r^2 \sim 3\pi\sigma^2 = \frac{6\pi K_{hor}}{w} z + S_f$$

For constant w ,

$$\frac{dV}{dz} = w\tau \frac{dS}{dz}$$

$$\frac{de}{dz} = -\frac{c_p \rho_a \theta}{g} N^2 - \frac{6\pi K_{hor}}{w^2 (S_f + 6\pi z K_{hor} / w)^2} P_f$$

Boundary condition: $e(0) = e_0$

The final height of the plume: $e(H_p) = 0$

MER scheme derivation (4)

Assume all parameters are constant

$$e = -\frac{c_p \rho_a \theta}{g} N^2 z + \frac{P_f}{w \left(S_f + \frac{6\pi K_{hor}}{w} z \right)}$$

$$\left\{ \begin{array}{l} e(H_p) = -\frac{c_p \rho_a \theta}{g} N^2 H_p + \frac{P_f}{w \left(S_f + \frac{6\pi K_{hor}}{w} H_p \right)} = 0 \\ \xi = S/S_f \\ \xi_p = 1 + \frac{6\pi H_p K_{hor}}{S_f w} \end{array} \right. \quad -\frac{c_p \rho_a \theta S_f^2 w N^2}{6\pi g K_{hor}} \xi_p^2 + \frac{P_f}{w} \xi_p + \frac{P_f}{w} = 0$$

$$-\frac{c_p \rho_a \theta S_f^2 w N^2}{6\pi g K_{hor}} (\xi_p^2 - \xi_p) + \frac{P_f}{w} = 0 \quad A = \frac{c_p \rho_a \theta w^2 S_f^2}{3\pi g K_{hor}}$$

$$\xi_p = \frac{1}{2} \left(1 + \sqrt{1 + \frac{8P_f}{AN^2}} \right) \Rightarrow H_p = f(P_f, N, \dots)$$

MER scheme derivation (5)

1. A has to be taken as a constant

$$S_f = 10^3 m^2 \quad w \sim 1m / s \quad K_{hor} \sim 1m^2 / s \quad A \sim 4 \times 10^9 Js$$

$$A = \frac{P_{f0}}{N_0^2} \quad P_{f0} = 10^6 W \quad N_0^2 = 2.5 \times 10^{-4} s^{-2}$$

2. The fire energy P_f spent on the air heating and the FRP observed from space are linearly related to the consumed biomass and close to each other.

3. Injection height will be proportional to FRP to the power of 0.5; but additional losses to friction and changing atmospheric and plume parameters will result a smaller power $\gamma < 0.5$

4. To avoid problems with $N^2 < 0$ inside the unstable ABL, take its FT value $N = N_{ft}$ ($z \sim 2H_{abl}$) but allow for some part of the ABL passed “freely” by adding a fraction of H_{abl} to H_p . In addition, instead of N_0^2/N^2 , use $\exp(-N^2/N_0^2)$, which for small N^2 limits the H_p growth by replacing N_0^2/N^2 with $1/(1+N^2/N_0^2)$. For large N^2 it quickly approaches zero, as one would expect for very stable stratification.

MER scheme derivation (6)

$$H_p = \alpha H_{abl} + \beta \left(\frac{FRP}{P_{f0}} \right)^\gamma \exp(-\delta N_{FT}^2 / N_0^2)$$

Here α is the part of ABL passed freely, β weights the contribution of the fire intensity, γ determines the power-law dependence on FRP, δ defines the dependence on stability in the FT.

$$\alpha < 1 \quad \beta > 0 \text{ m} \quad \gamma < 0.5 \quad \delta \geq 0$$

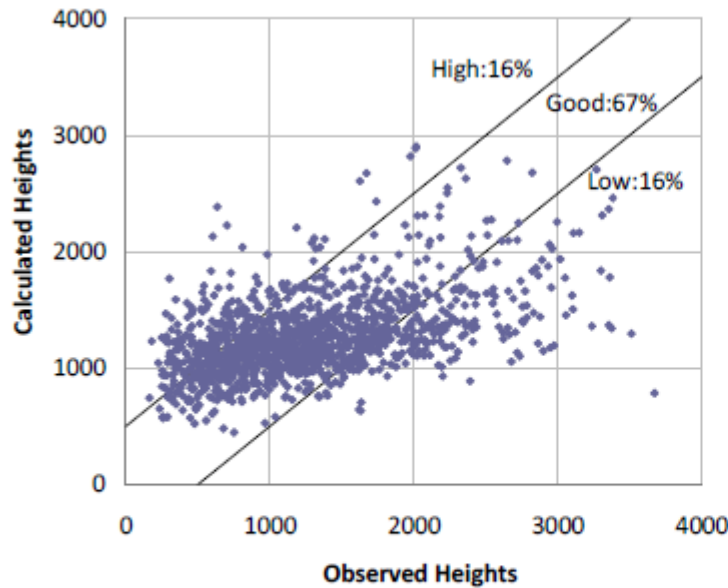
Determine the constants in this equation was based on the learning subset of the Multi-angle Imaging SpectroRadiometer (MISR) fire observations (70% of the MISR collection, 1278 fires)

$$J_R = \sum_{i=1}^{N_{fires}} \Theta \left(\left| H_p^{obs}(i) - H_p^{mdl}(i) \right| - \Delta h \right)$$
$$\Theta(x) = \begin{cases} 0, & x \leq 0 \\ 1, & x > 0 \end{cases}$$

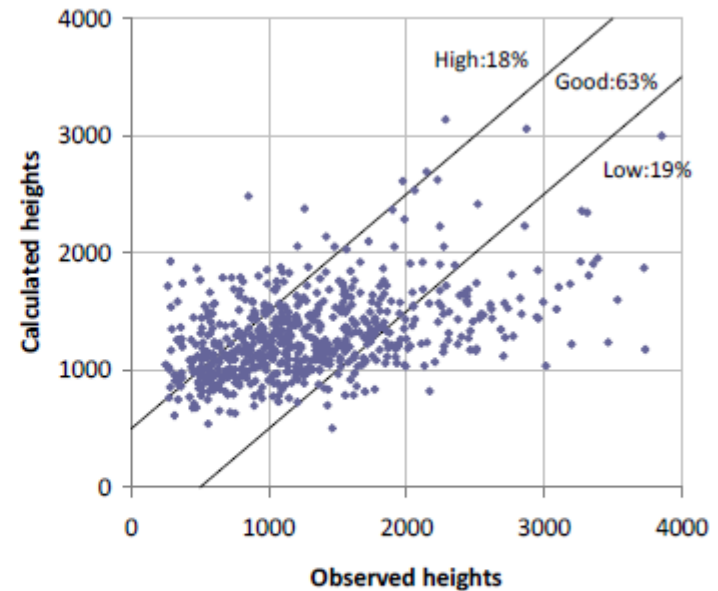
Here Δh is the desired accuracy of the prediction (500 m), N_{fires} is the number of fires in the subset, H_{obs} and H_{mdl} are the observed and predicted plume top heights of the i -th fire.

MER scheme derivation (7)

$$\alpha = 0.24 \quad \beta = 170m \quad \gamma = 0.35 \quad \delta = 0.6$$



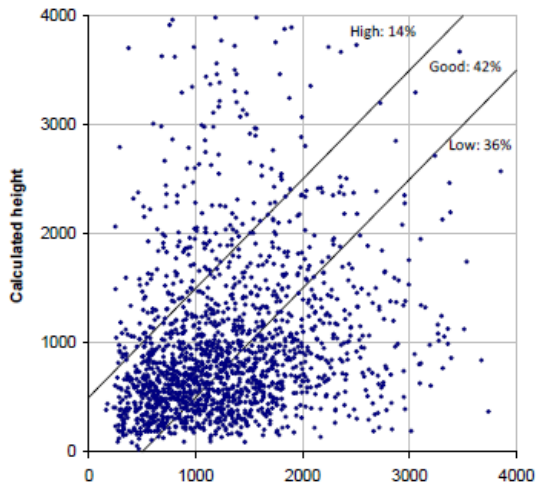
(a) Learning subset, Eqs. (10, 13)



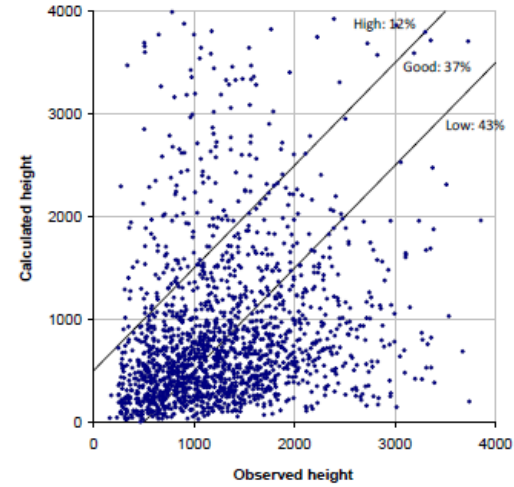
(b) Control subset, Eqs. (10, 13)

Fig. 1. Comparison of predictions of the formula (10) with the observed H_p for the learning (panel a) and control (panel b) subsets. Parameter values (Eq. 13). Unit = [m].

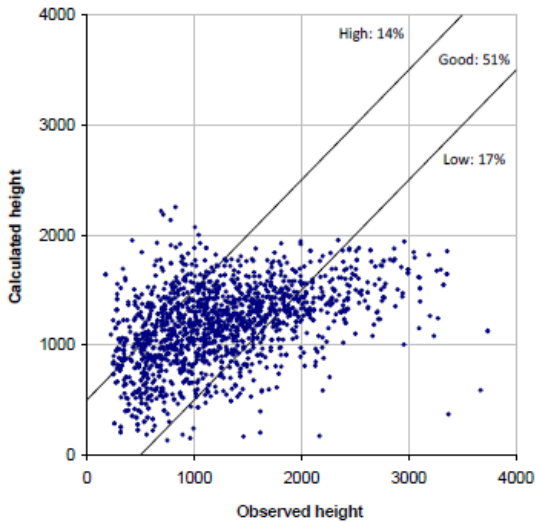
Comparison between different schemes



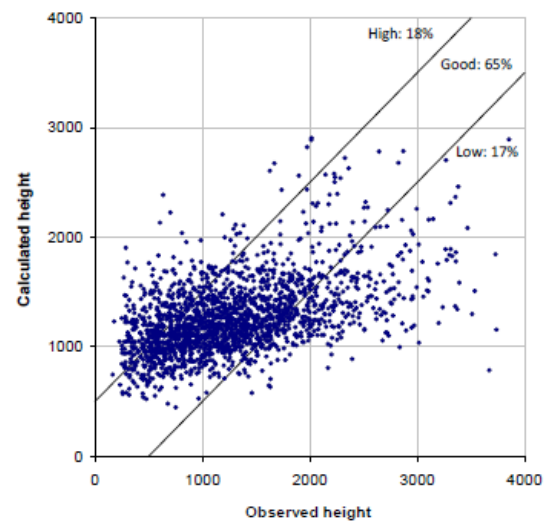
(a) Formulations B69



(b) Formulations B84



(c) BUOYANT model (1574 out of 1914 cases)



(d) Formula (10) with parameters (Eq. 13)

Fig. 2. Comparison of B69 (Eq. 17), B84 (Eq. 18), BUOYANT, and formula (10, 13) for the whole MISR set.

Contributions of different components

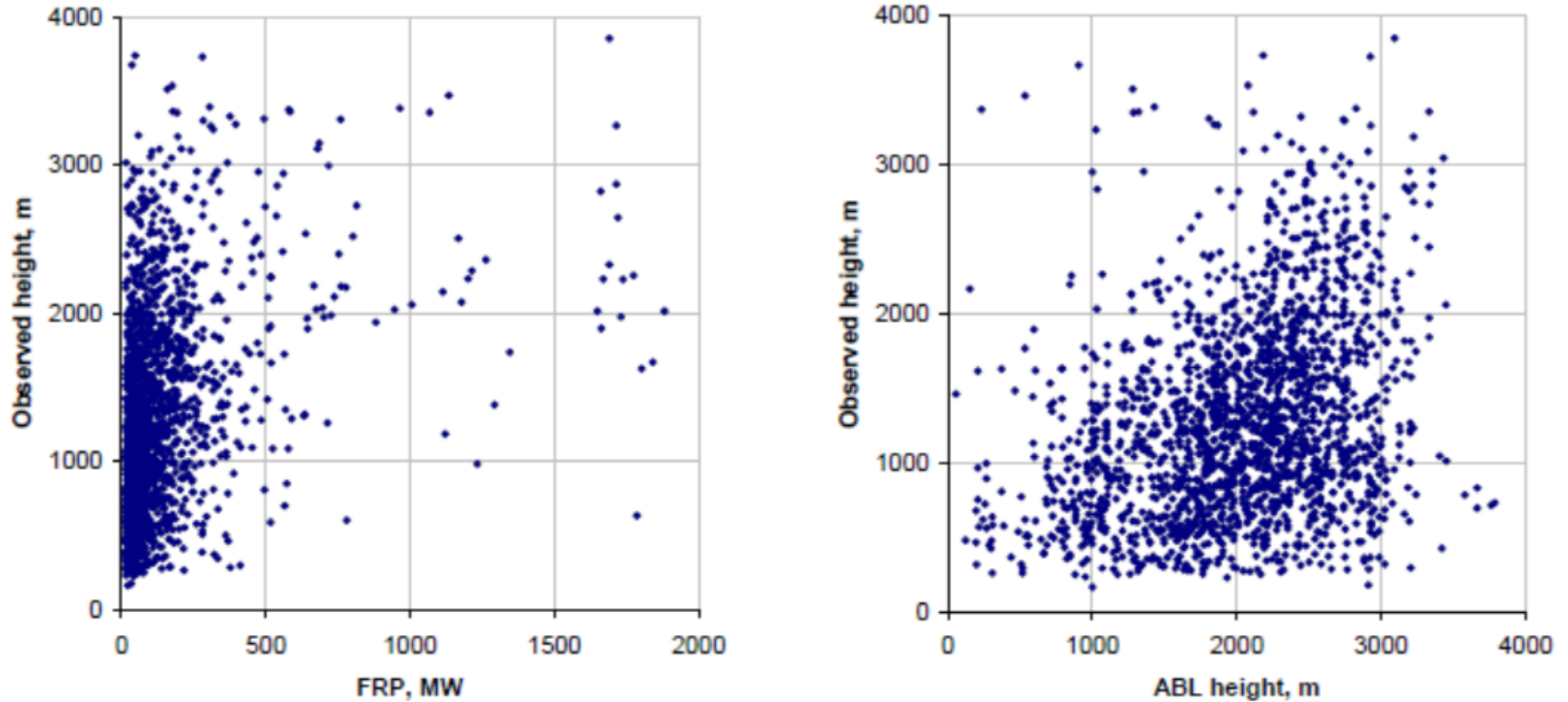


Fig. 3. Correlation of the observed plume height and individual components of the formula (10, 13): boundary layer height and FRP.

MER scheme application: wildfire emission heights and vertical profiles (1) – evaluation of MER scheme

Include fires in Africa and Borneo, which extended the previous evaluation towards savannah and tropical forests

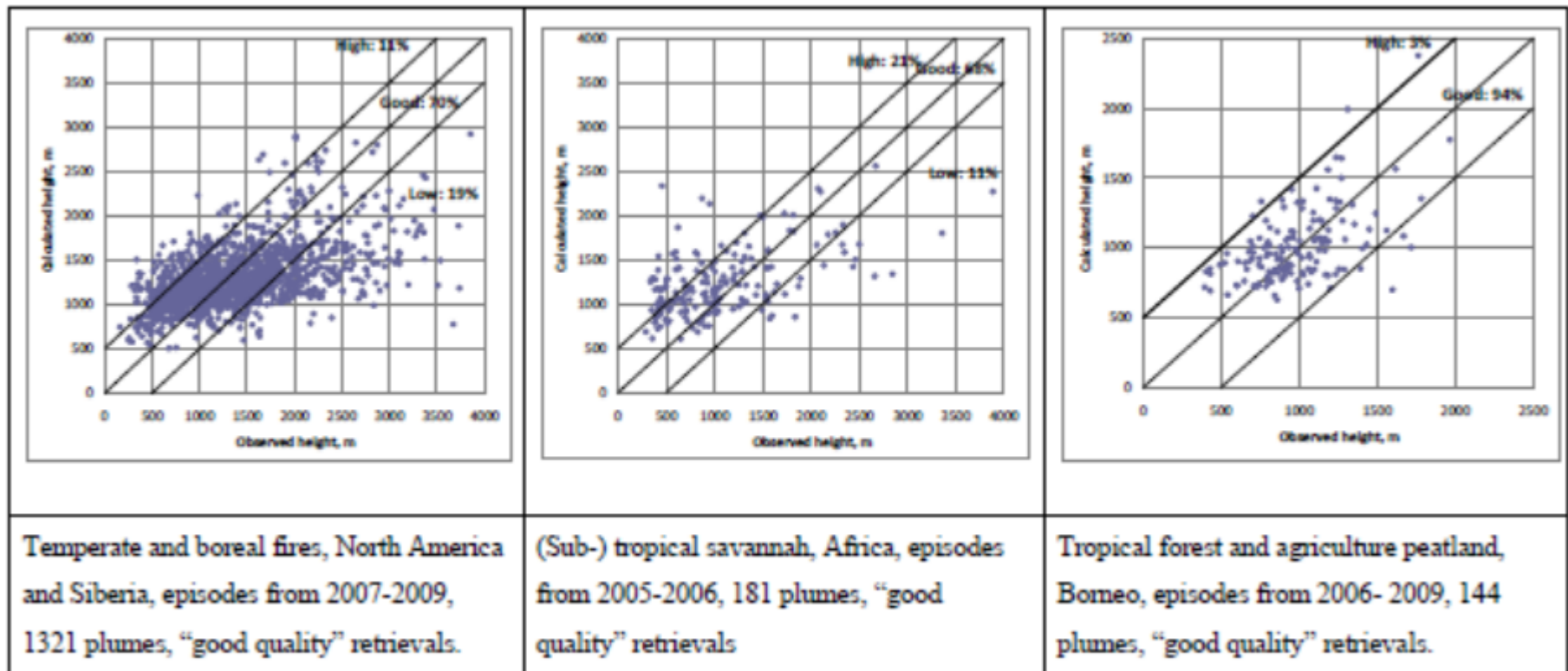


Fig. 1. Global evaluation of plume-top formulations of Sofiev et al. (2012) against MISR data. Unit = [m].

Diurnal cycle of fire intensity

Geo instrument SEVIRI onboard the Meteosat MSG satellite: high temporal resolution (about 15 min)

$$M.(n_i, l) = a_0 + \sum_{k=1}^3 a_k(l) \cdot \cos\left(\frac{k}{12} \pi n_t\right) + \sum_{k=1}^3 b_k(l) \cdot \sin\left(\frac{k}{12} \pi n_t\right)$$

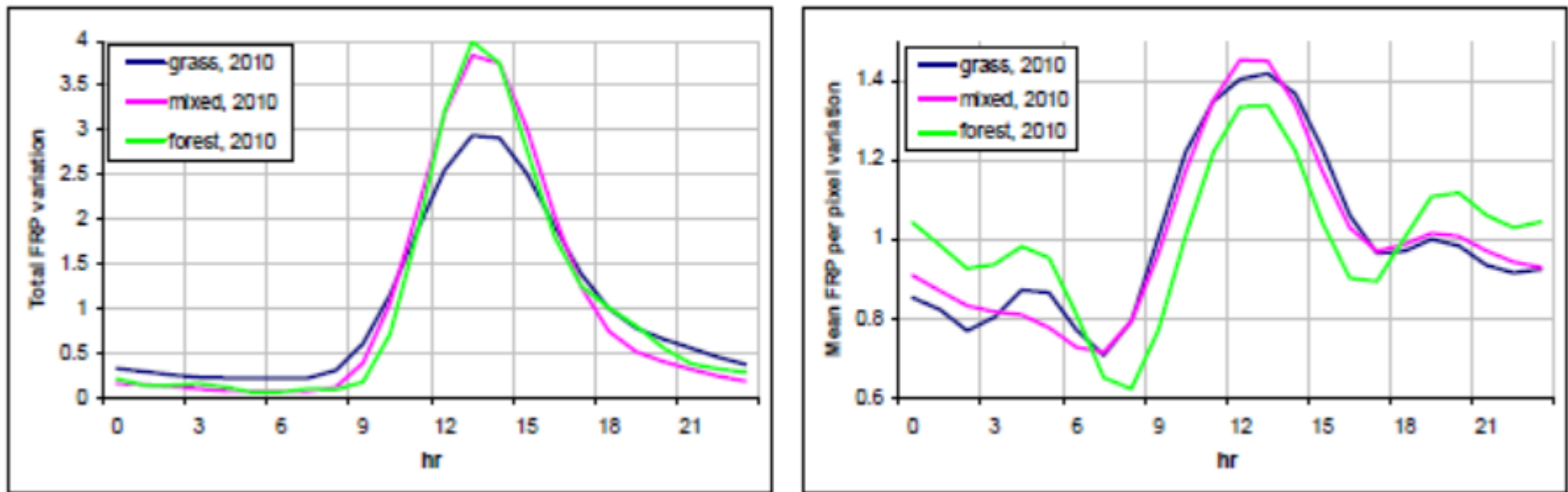


Fig. 2. Diurnal variations of total FRP (left), mean FRP per GEO-pixel (right). SEVIRI, mean over 2010. Relative unit.

Wild land fire emissions

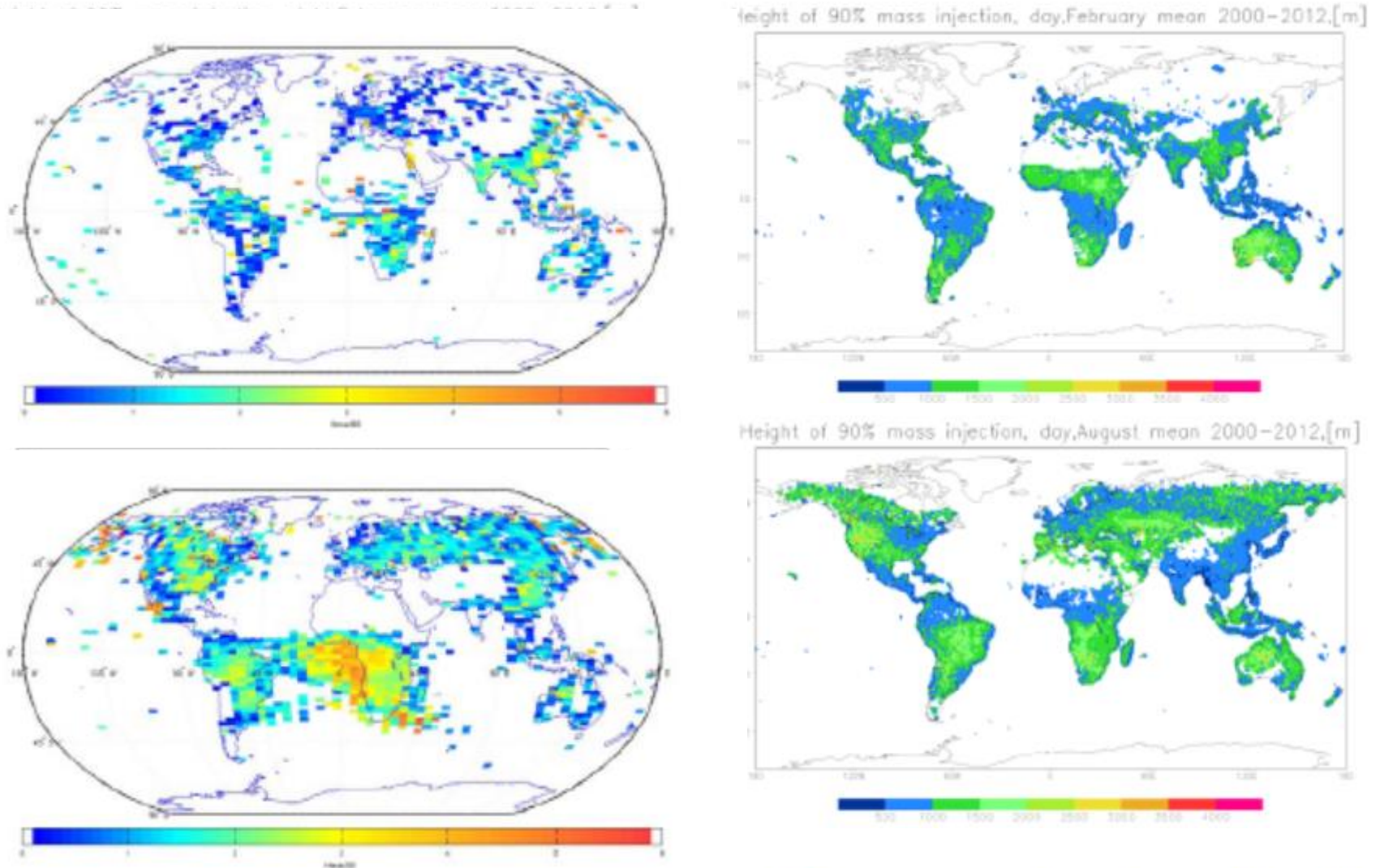


Fig. 4. injection height for 90 % of mass for night (left) and day (right) for February (top) and August (bottom). Unit = [m].

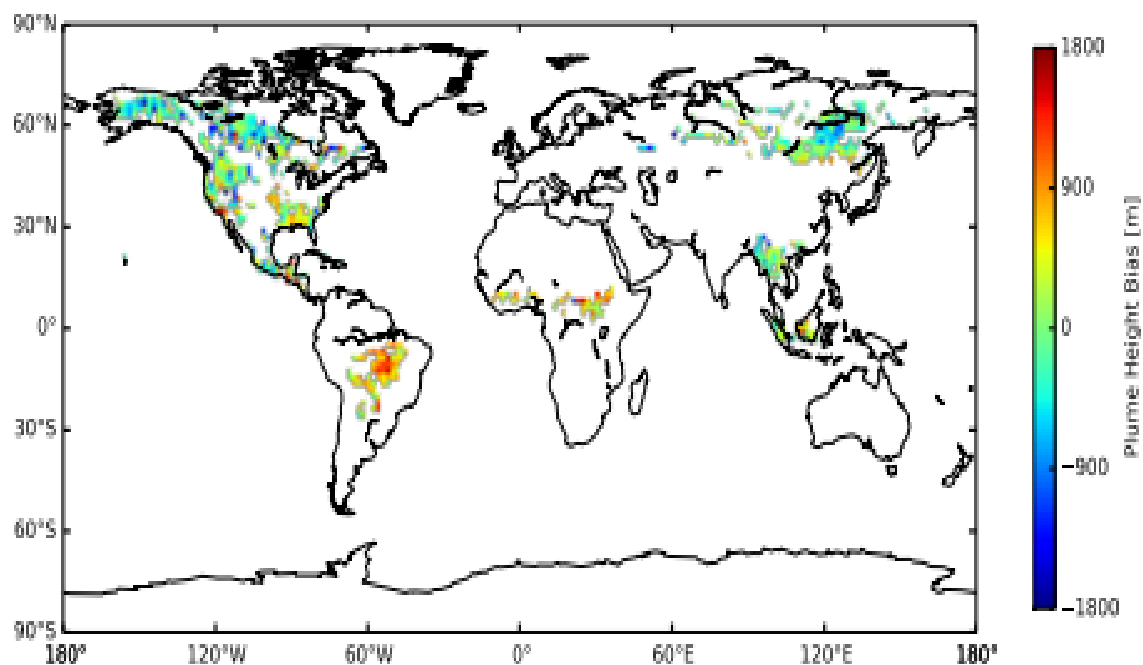
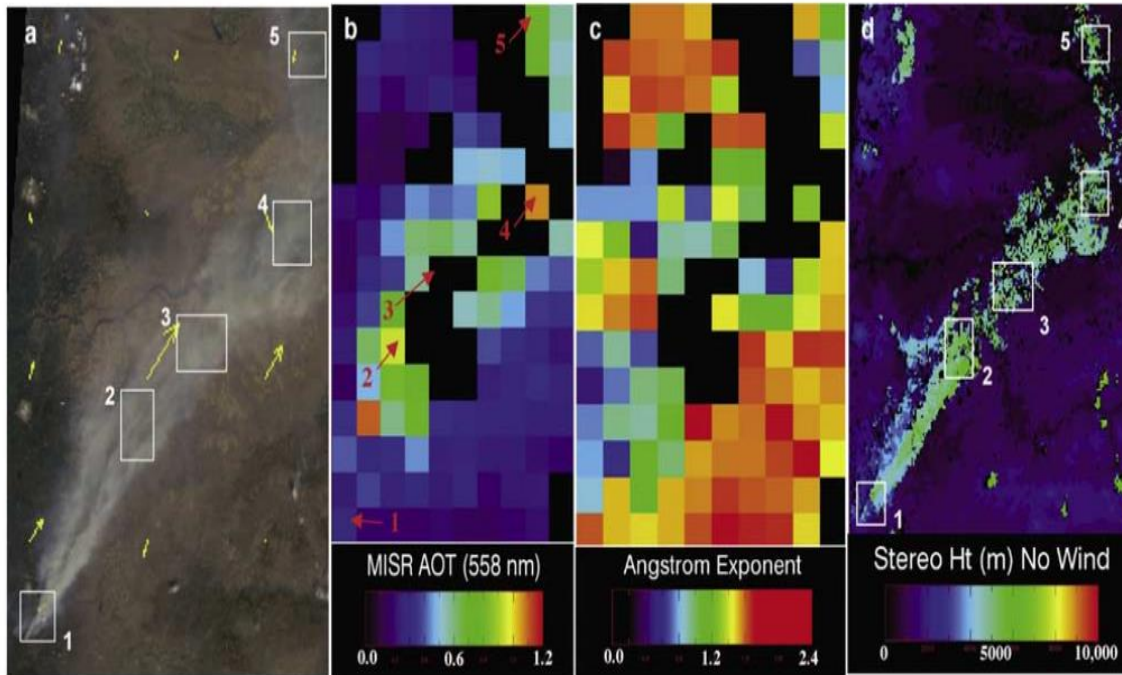
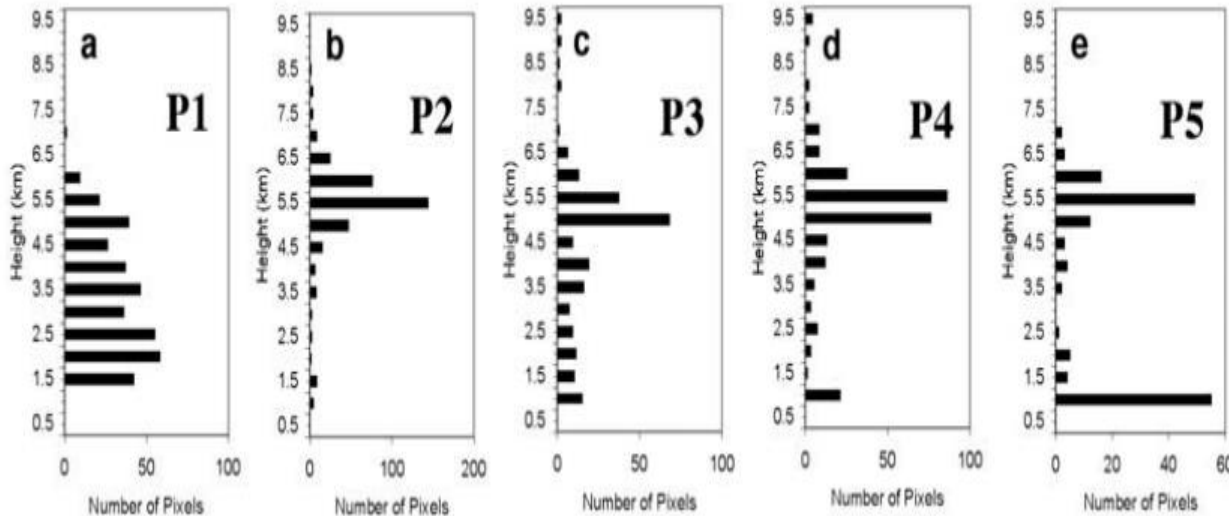


Figure 5. Mean plume height bias of simulation EVAL-SOFIEV-1 for 2001–2009 compared to the observational MPHP data set (EVAL-SOFIEV-1 minus MPHP). Blue colors indicate underestimation of plume heights by the model, red colors indicate overestimation of plume heights by the model. The large majority of grid boxes contains more than one individual plume; in these cases averaged biases are shown. The large areas of white colors, e.g. in Europe and Australia, represent the limited global coverage of the MPHP data set as no plumes are available in these regions.



➤ MISR plume height

- Pixel resolution : 1.1 km
- Vertical resolution: 500m
- A question is how to match MISR to MODIS hotspots



➤ 3D Simulation: ATHAM

- Location: Chisholm Fire, May 28, 2001, Canada
- Spread rate: 5.4 km/h; 7×10^7 MJ in 7 hr
- Resolution: 100m x 50m in horizontal, 50m in vertical
- Fire: $250,000 \text{ kw s}^{-1}$ as fire front line. Heat flux 100 kw m^{-2}
- Maximum height: 12 km

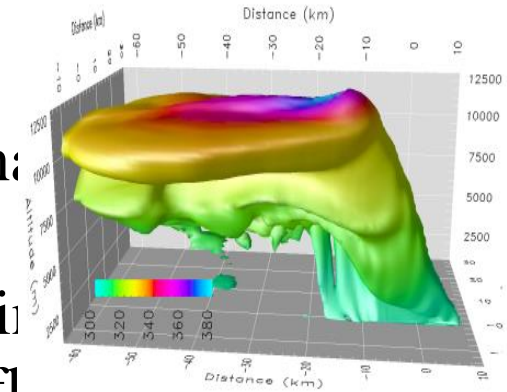


Fig. 4. Spatial distribution of the $150 \mu\text{g m}^{-3}$ -isosurface of the simulated aerosol mass distribution after 40 min of simulation time. The color coding represents the potential temperature.

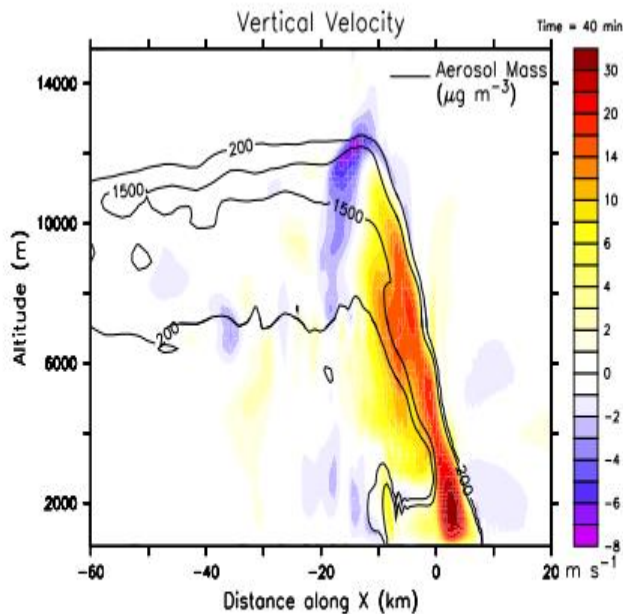


Fig. 10. Simulated updraft velocity (color coding) and aerosol mass concentration (contour lines) after 40 min along the cross section at $y=0$.

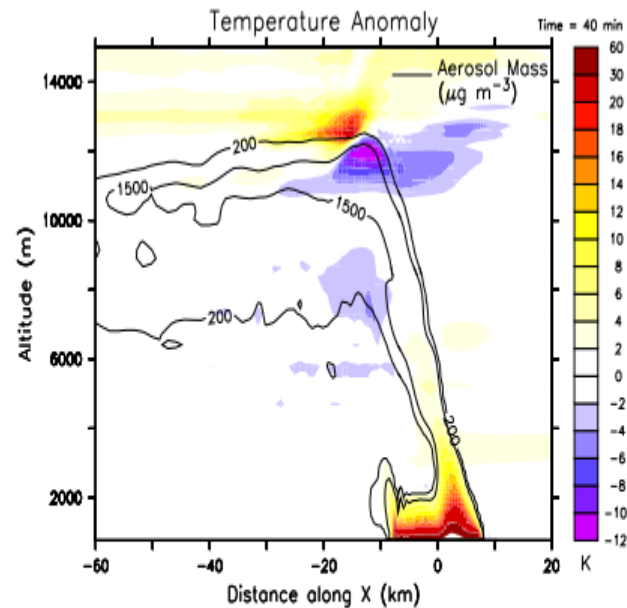
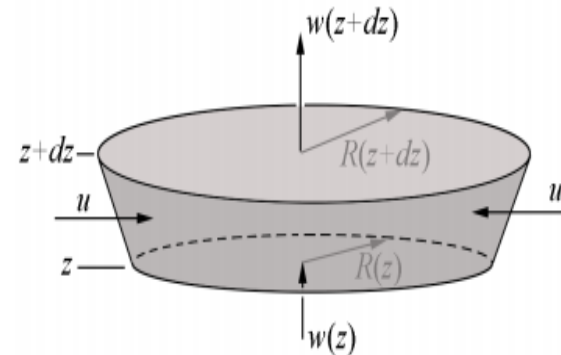


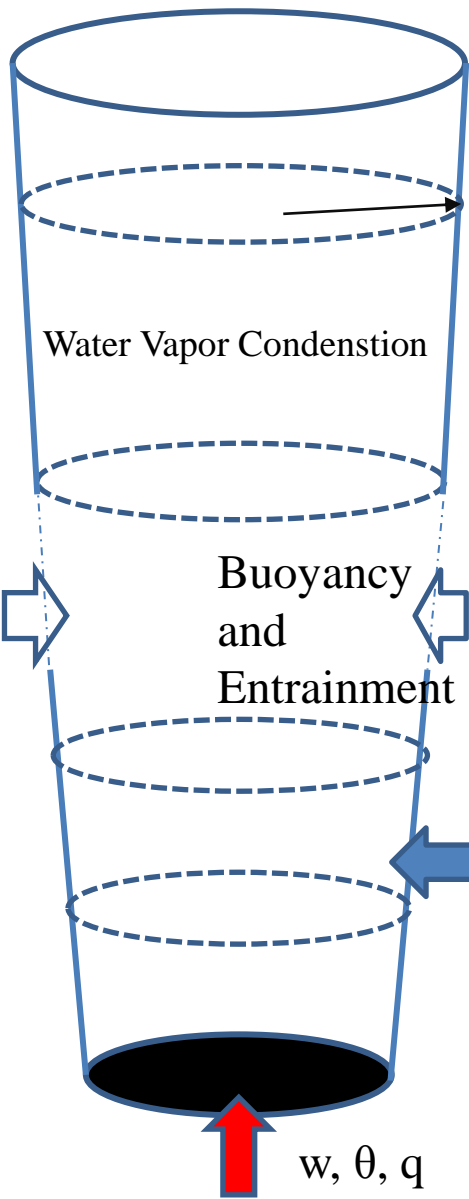
Fig. 11. Simulated temperature anomaly after 40 min along the cross section at $y=0$. Shown is the difference between the simulated and the initialized ambient temperature. Negative (positive) temperature anomalies are shown in blue (red).

1D Plume-Rise Model

- Governing Equations
- Boundary Conditions
- Plume Top Criteria
- Wind effect
- Applications



$$\frac{d\pi R^2 w}{dz} = 2\pi R u; \text{ where } u = \alpha w$$



Plume Top Criteria: $W < 1 \text{ m/s}$

Radius varies with height

Cloud Physics:

Kessler parameterization, 1969

Ice formation:

Ogura and Takahashi, 1971

Autoconversion: Berry, 1967

Buoyancy
and
Entrainment

Governing Equations
Simpson and Wiggert, 1969

Wind Effect

Freitas et al., 2010

Fire boundary:

Morton, Taylor and Turner;

1955

Bottom Boundary:

Momentum, Heat and Water Flux

➤ Governing Equations

$$\frac{\partial w}{\partial t} + w \frac{\partial w}{\partial z} = \frac{1}{1+\gamma} g B - \frac{2\alpha}{R} w^2 + \frac{\partial}{\partial z} \left(K_m \frac{\partial w}{\partial z} \right) \quad (1)$$

$$\begin{aligned} \frac{\partial T}{\partial t} + w \frac{\partial T}{\partial z} = & -w \frac{g}{c_p} - \frac{2\alpha}{R} |w| (T - T_e) \\ & + \frac{\partial}{\partial z} \left(K_T \frac{\partial T}{\partial z} \right) + \left(\frac{\partial T}{\partial t} \right)_{\text{microphysics}} \end{aligned} \quad (2)$$

$$\begin{aligned} \frac{\partial r_v}{\partial t} + w \frac{\partial r_v}{\partial z} = & -\frac{2\alpha}{R} |w| (r_v - r_{ve}) \\ & + \frac{\partial}{\partial z} \left(K_T \frac{\partial r_v}{\partial z} \right) + \left(\frac{\partial r_v}{\partial t} \right)_{\text{microphysics}} \end{aligned} \quad (3)$$

$$\begin{aligned} \frac{\partial r_c}{\partial t} + w \frac{\partial r_c}{\partial z} = & -\frac{2\alpha}{R} |w| r_c \\ & + \frac{\partial}{\partial z} \left(K_T \frac{\partial r_c}{\partial z} \right) + \left(\frac{\partial r_c}{\partial t} \right)_{\text{microphysics}} \end{aligned} \quad (4)$$

Freitas et al., 2007

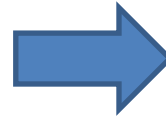
➤ Simpson and Wiggert, 1969

$$\frac{dw}{dt} = w \frac{dw}{dz} = \frac{d}{dz} \left(\frac{w^2}{2} \right) = \frac{gB}{1+\gamma} - \frac{3}{8} \left(\frac{3}{4} K_2 + C_D \right) \frac{w^2}{R} \quad (1)$$

$$\text{buoyancy} = gB = \frac{g[\Delta T_v - \Delta T_v (\text{LWC})]}{T_v (\text{env})} \quad (3)$$

TABLE 1.—Parameters of the EMB cumulus models

Parameter	Meaning	EMB 65	EMB 68	Remarks
K_2	Entrainment.....	0.55.....	0.65.....	Lab. value 0.71
C_D	Aerodynamic drag coefficient	0.506.....	0.....	Solid-sphere value=1.125
γ	Virtual mass coefficient	0.....	0.5.....	Lab. value 0.5
LWC	Liquid water retained	½ condensate.	Falloutscheme ..	Much improved in EMB 68



➤ Governing Equations

$$\frac{\partial w}{\partial t} + w \frac{\partial w}{\partial z} = \frac{1}{1+\gamma} gB - \frac{2\alpha}{R} w^2 + \frac{\partial}{\partial z} \left(K_m \frac{\partial w}{\partial z} \right) \quad (1)$$

$$\begin{aligned} \frac{\partial T}{\partial t} + w \frac{\partial T}{\partial z} = & -w \frac{g}{c_p} - \frac{2\alpha}{R} |w| (T - T_e) \\ & + \frac{\partial}{\partial z} \left(K_T \frac{\partial T}{\partial z} \right) + \left(\frac{\partial T}{\partial t} \right)_{\text{microphysics}} \end{aligned} \quad (2)$$

$$\begin{aligned} \frac{\partial r_v}{\partial t} + w \frac{\partial r_v}{\partial z} = & -\frac{2\alpha}{R} |w| (r_v - r_{ve}) \\ & + \frac{\partial}{\partial z} \left(K_T \frac{\partial r_v}{\partial z} \right) + \left(\frac{\partial r_v}{\partial t} \right)_{\text{microphysics}} \end{aligned} \quad (3)$$

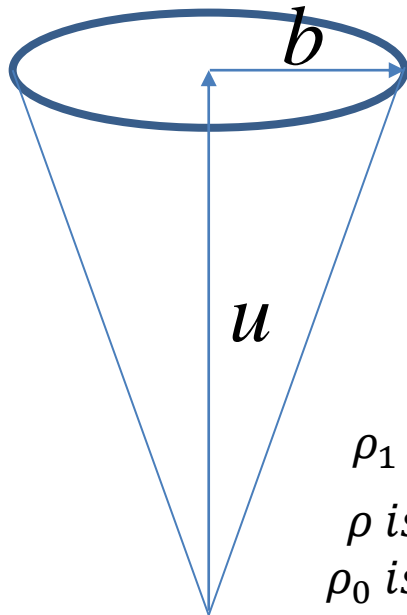
$$\begin{aligned} \frac{\partial r_c}{\partial t} + w \frac{\partial r_c}{\partial z} = & -\frac{2\alpha}{R} |w| r_c \\ & + \frac{\partial}{\partial z} \left(K_T \frac{\partial r_c}{\partial z} \right) + \left(\frac{\partial r_c}{\partial t} \right)_{\text{microphysics}} \end{aligned} \quad (4)$$

Freitas et al., 2007

➤ Bottom Boundary: turbulent gravitational convection

Morton, Taylor and Turner; 1955

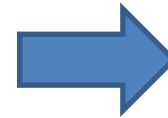
- (i) $\frac{d}{dx}(\pi b^2 u) = 2\pi b \alpha u$ (volume),
- (ii) $\frac{d}{dx}(\pi b^2 u^2 \rho) = \pi b^2 g(\rho_0 - \rho)$ (momentum),
- (iii) $\frac{d}{dx}[\pi b^2 u(\rho_1 - \rho)] = 2\pi b \alpha u(\rho_1 - \rho_0)$ (density deficiency),



ρ_1 is $\rho_0(0)$
 ρ is inside density
 ρ_0 is outside density

If outside density is uniform, there is an analytical solution

$$b^2 u g \frac{\rho_1 - \rho}{\rho_1} = Q = \text{constant}$$



$$F = \frac{g^{\mathfrak{R}}}{c_p P_e} E R^2$$

$$w_0 = \frac{5}{6\alpha} \left(\frac{0.9\alpha F}{z_v} \right)^{1/3}$$

$$\frac{\Delta\rho_0}{\rho_{e,0}} = \frac{5}{6\alpha} \frac{F}{g} \frac{z_v^{-5/3}}{(0.9\alpha F)^{1/3}}$$

$$T_0 = \frac{T_{e,0}}{1 - \frac{\Delta\rho_0}{\rho_{e,0}}}$$

➤ Bottom Boundary: Two Questions

if
$$\frac{\rho_0 - \rho}{\rho_0} = \frac{T - T_0}{T_0}$$

then
$$T = \frac{\rho_0 - \rho}{\rho_0} T_0 + T_0$$

not
$$T_0 = \frac{T_{e,0}}{1 - \frac{\Delta\rho_0}{\rho_{e,0}}}$$

$$\frac{d}{dx} [\pi b^2 u (\rho_1 - \rho)] = 2\pi b \alpha u (\rho_1 - \rho_0)$$

$$b^2 u g \frac{\rho_1 - \rho}{\rho_1} = Q = \text{constant}$$

conservation of density deficiency (the equivalent of heat)

All heat convert to density deficiency, but how about kinetic energy

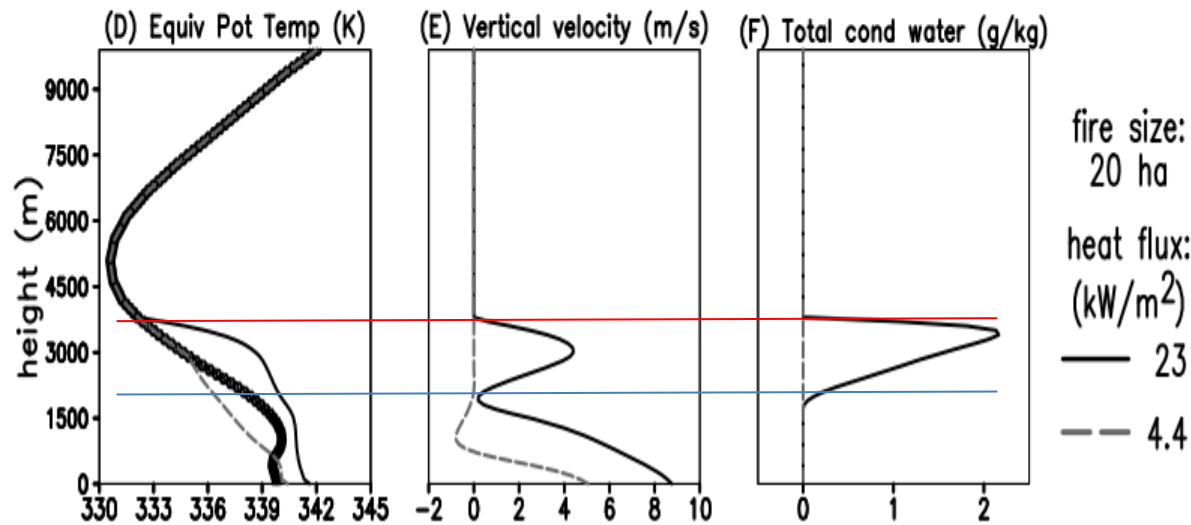
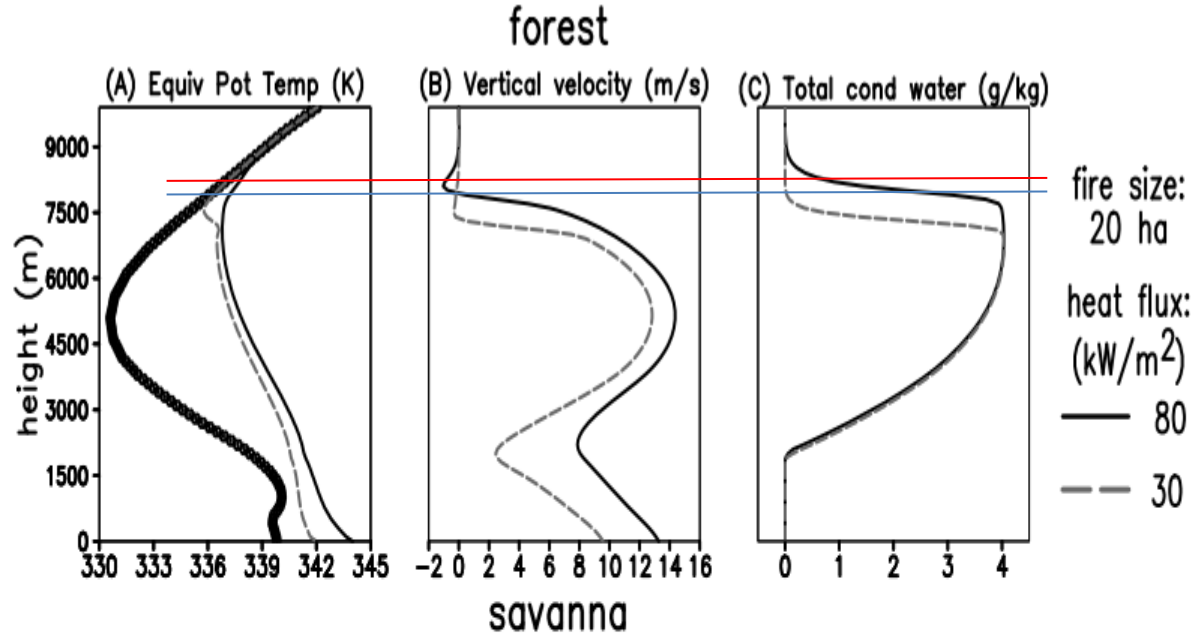
Suggestions:

Keep the w small and recalculate the α and T

$$w_0 = \frac{5}{6\alpha} \left(\frac{0.9\alpha F}{z_v} \right)^{1/3}$$

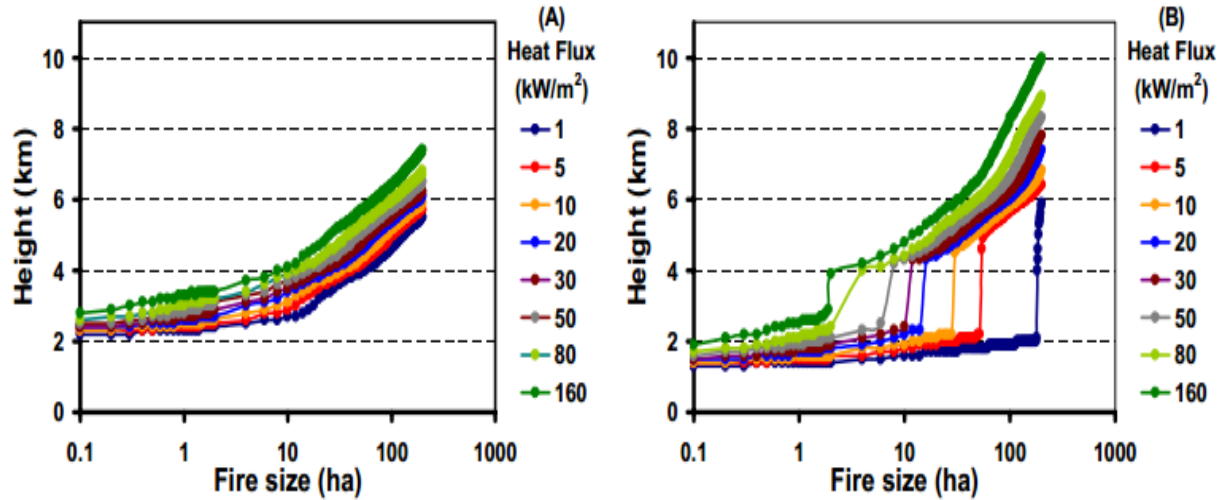
$$\frac{\Delta\rho_0}{\rho_{e,0}} = \frac{5}{6\alpha} \frac{F}{g} \frac{z_v^{-5/3}}{(0.9\alpha F)^{1/3}}$$

➤ Bottom Boundary: Plume Top Criteria



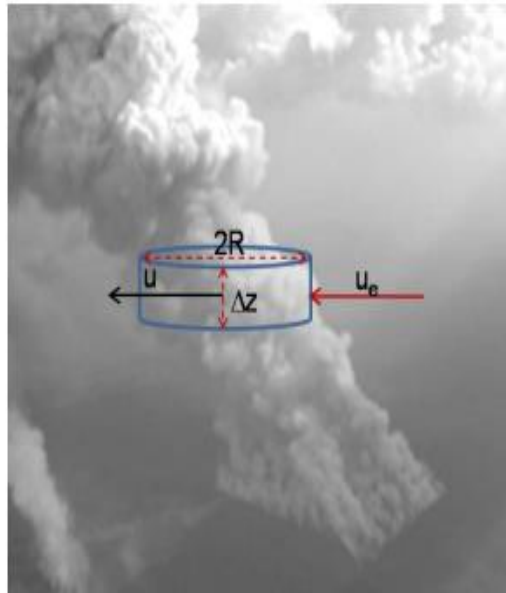
- $w = 1 \text{ m/s}$
- Zero buoyancy

➤ Condensation Effect

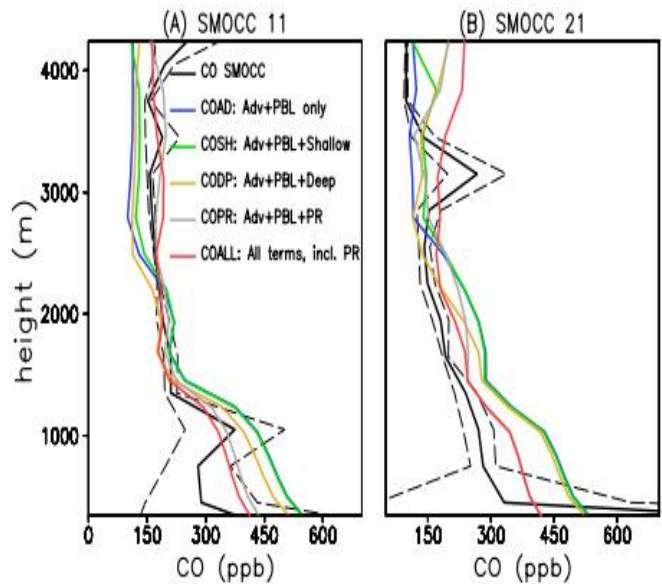
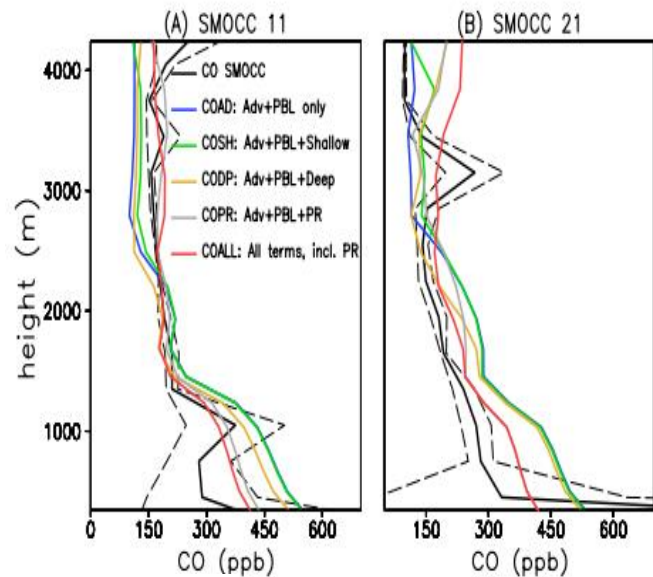
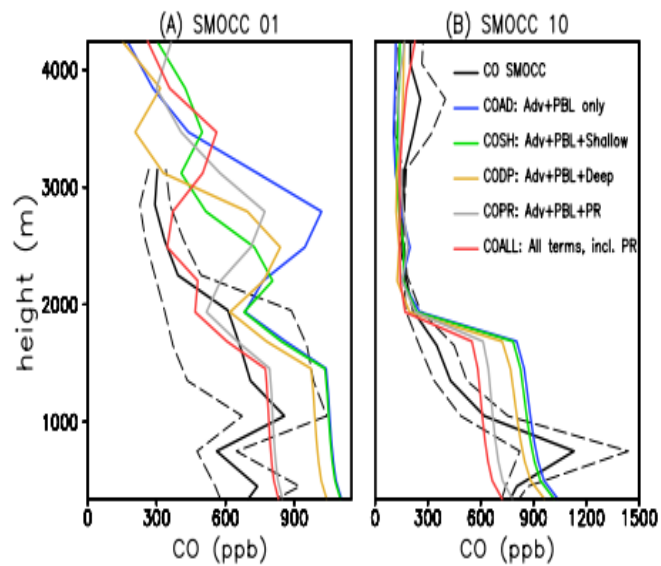


➤ Wind Effect

$$\delta_{entr} = \frac{2}{\pi R} (u_e - u).$$



➤ Application



Conclusions

- A new methodology for the estimation of plume rise height from wild-land fires is proposed and evaluated. Two thirds of its predictions deviated from the MISR observations by less than 500m.
- Set up a global fire emission distribution map.
- The entrainment term in 1D plume-rise model is designed for free troposphere not boundary layer.
- The bottom boundary condition does not conserve the energy.
- The plume top criteria is problematic.
- The condensation parameterization needs further investigation.

References

Gary A. Briggs (1965) A Plume Rise Model Compared with Observations, *Journal of the Air Pollution Control Association*, 15:9, 433-438, DOI: 10.1080/00022470.1965.10468404

M. Sofiev, T. Ermakova, and R. Vankevich (2012) Evaluation of the smoke-injection height from wild-land fires using remote-sensing data, *Atmospheric Chemistry and Physics*, 12, 1995-2006, DOI: 10.5194/acp-12-1995-2012

M. Sofiev, R. Vankevich, T. Ermakova, and J. Hakkarainen (2013) Global mapping of maximum emission heights and resulting vertical profiles of wildfire emissions, *Atmospheric Chemistry and Physics*, 13, 7039-7052, DOI: 10.5194/acp-13-7039-2013

Scott L. Goodrick, Gary L. Achtemeier, Narasimhan K. Larkin, Yongqiang Liu and Tara M. Strand (2012) Modelling smoke transport from wildland fires: a review, *International Journal of Wildland Fire*, 22, 83-94

Freitas, Saulo R., et al. "Including the sub-grid scale plume rise of vegetation fires in low resolution atmospheric transport models." *Atmospheric Chemistry and Physics* 7.13 (2007): 3385-3398.

Freitas, S. R., et al. "Technical Note: Sensitivity of 1-D smoke plume rise models to the inclusion of environmental wind drag." *Atmospheric Chemistry and Physics* 10.2 (2010): 585-594.

Simpson, Joanne, and Victor Wiggert. "Models of precipitating cumulus towers." *Monthly Weather Review* 97.7 (1969): 471-489.

Trentmann, J., et al. "Modeling of biomass smoke injection into the lower stratosphere by a large forest fire (Part I): reference simulation." *Atmospheric Chemistry and Physics* 6.12 (2006): 5247-5260.

Turner, John Stewart, and John Stewart Turner. *Buoyancy effects in fluids*. Cambridge University Press, 1979.

Veira, A., et al. "Fire emission heights in the climate system—Part 1: Global plume height patterns simulated by ECHAM6-HAM2." *Atmospheric Chemistry and Physics Discussions* 15.5 (2015): 6645-6693.